

An Investigation of Multi-Porous Silicon Gas Sensor

Dr. Alwan M. Alwan 

Applied Physes Department, School of App Laid Science, University of Technology/Bagdad
Email: ALKRZM@yahoo.com

Received on: 19/ 3/2013 & Accepted on: 5/12/2013

BSTRACT

Efficient porous silicon organic vapors sensors were fabricated by employing a multi-porous silicon layer (mPSi) within (Au/mPSi/n-Si/Au) sandwich structures. Based on the morphological nature and the resistivity of resulting (mPSi), the mechanism of current flow in the sensor was analyzed. The SEM images of (mPSi) layer reflect the formation of complex porous and mud-like structures. The mud-like structure consists of connected and non-connected trenches while the pore-like structure consists of different pore sizes formed inside this structure. The current response is governed by the silicon channel between the adjacent mud's rather than the silicon nanowires between the adjacent pores.

تقسي المتحسسات الغازية للسليكون المسامي المتعدد المسامات

الخلاصة

تم تحضير متحسس كفاء للابخرة العضوية باستخدام طبقات السليكون المتعدد المسامية (mpsi) ضمن تركيب شرائحي من (Au/mpsi/ n-si/Au) . الية تدفق التيار ضمن المتحسس تم تحليلها بالاعتماد على الطبيعة الطوبوغرافية و مقاومة طبقة السليكون المسامي المتعدد المسامية . اظهرت صور المجهر الالكتروني الماسح (SEM) تكون تركيب مسامي معقد يحوي على تركيب مشابه لكل من الرقع الطينية والفجوات.

تفصل بين الرقع مجموعة من الاخاديد المتصلة و غير المتصلة فيما بينها بينما تركيب الفجوات يتكون من مجموعة من الفجوات المختلفة الابعاد و تقع هذه ضمن الرقعة الواحدة . ان استجابة المتحسس للتيار تحكمها قناة السليكون الواقعة بين الرقع بدلا من الاسلاك النانوية الواقعة بين الفجوات المتجاورة.

INTRODUCTION

Porous silicon (Psi) is an open silicon skeletal matrix formed by electrochemical or photochemical etching of silicon substrate in a solution containing hydrofluoric acid (HF) [1]. By controlling the etching conditions such as (current density, time, illumination intensity and illumination wavelength), and substrate doping, the morphology and porosity (percentage of the void space in the porous matrix) of a Psi layer can be controlled. (Psi) is well-suited as an alternative material for chemical and biosensors [2,3]. The use of porous instead of planar silicon as substrate material provides many advantages due to the large surface to volume ratio that can reach $500\text{m}^2 /$

cm^{-3} . The porous silicon /silicon substrate junction had been used for sensing applications as gas sensors based upon the increase in current due to the dipole moment of the gas [4,5] or due to charges trapped on the dangling bonds associated with the silicon /porous silicon interface [6]. In previous studies, (Psi) porosity gradient was discussed primarily as artifacts in standard constant current etching [7], as a characterization tool for optoelectronics studies [8] and for **optical** filter applications [9] and also for silicon solar cell applications as an antireflection coating [10]. In the present work, the properties of a multi-porous silicon layer (mPSi) used as gas sensor by fabricating (Au/mPSi/n-Si/Au) sandwich structures is investigated. The electrical response of this sensor is discussed based on the analysis of the surface morphology of the (mPSi) by means of SEM micro images.

EXPERIMENTAL WORK

A multi-porous silicon layer was fabricated by etching of n-type silicon wafer of (110) orientation and (1-10 $\Omega\cdot\text{cm}$) resistivity in a mixture of ($\text{H}_2\text{O}:\text{HF}:\text{C}_2\text{H}_5\text{OH}=1:1:2$). The multi-porous layer was made using laser-assisted etching process which employed 405 nm diode laser at different illumination intensities at steps of 20 mW/cm^2 and 100 mW/cm^2 and fixed etching time of 7 min. The etching process was materialized in a specially designed cell that comprises two – electrode system as an anode and a mesh as cathode. The experiment was conducted at room temperature and its setup is shown in the Figure (1).

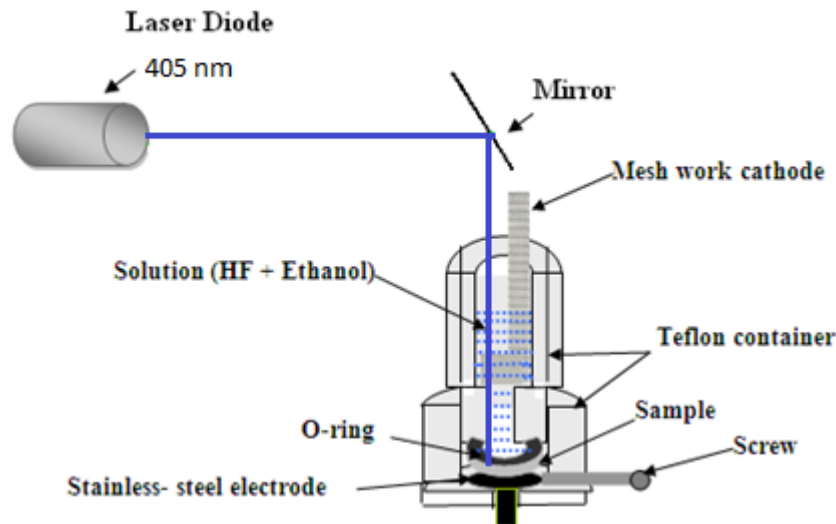


Figure (1) Schematic diagram of the Laser assisted etching system.

The cell provides a porous silicon layer of uniform cross sectional area. This uniformity is recommended for the application of (Psi) in the field of gas sensors. The cross section of the home-made cell is shown in Figure (1), in which a mesh cathode with an aperture size of (2*2mm) was used. The values of the porosity and the thickness of the porous layer are determined gravimetrically. The SEM measurements were carried out in

the school of material engineering at the University Sains Malaysia in Penang. The current –voltage characteristics were studied by evaporating an Ohmic contact on the back side of the sample using a thick gold electrode. On the top etched side of the sample, a thin gold film of 15-20 nm thickness was evaporated directly on the porous layer in order to produce (Scotty-like) diode. Figure (2) shows the measurement set-up for vapors sensing. As shown in this figure, the gas vaporized from diluted organic solutions (ethanol and methanol) was warmed up by a heater and was injected through a tube into a chamber with N₂ gas as a carrier gas. Every measurement was carried out after 60 sec of exposure time to the gas. The current –voltage measurements were carried out using fine dc power supply and 8846A Fluke 6-1/2 Digit precision multimeter.

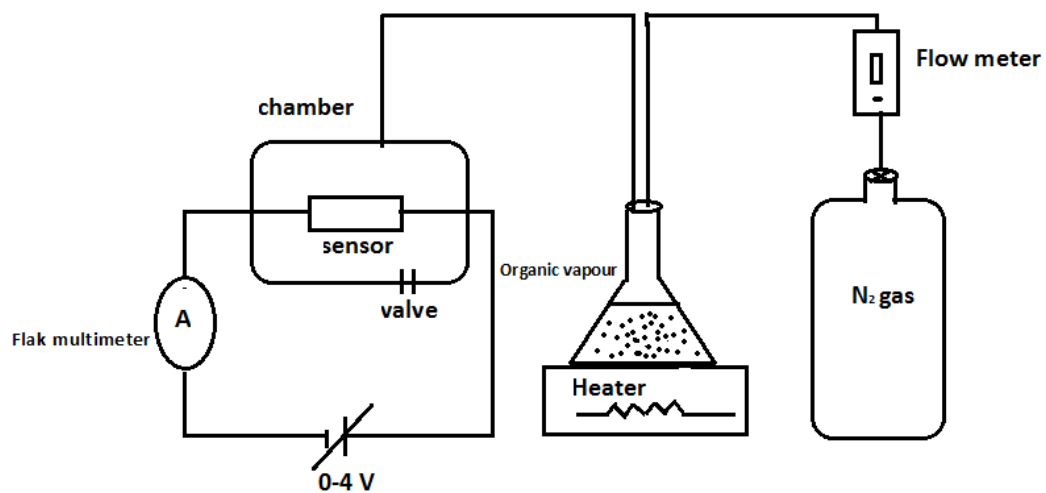


Figure (2) Schematic diagram of the gas sensing measurements.

RESULTS AND DISCUSSION

For (mPsi) sample etched at two steps with laser intensities of 40mW/cm² and 20mW/cm², the porosity of the multi-porous silicon layer (49%) and the layer thickness (3.5 μm) were determined by using gravimetric measurements. These values are (68%) and (7.8 μm) respectively, and calculated based on Equations (1) and (2) respectively.

$$\gamma(\%) = \frac{m_1 - m_2}{m_1 - m_3} \quad \dots (1)$$

Where (m₁) is the weight of silicon wafer before etching process, (m₂) is the weight just after etching, and m₃ is the weight of the sample after removing the porous layer. While the thickness of the porous layer (d) is determined by using gravimetric measurements.

$$d = \frac{m_1 - m_2}{A \times \rho} \quad \dots (2)$$

Where (A) corresponds to the illumination area (cm^2) and (ρ) to the density of bulk silicon ($\rho = 2.33 \text{ g/cm}^3$).

The etching process was carried out at four steps using laser intensities of 100, 80, 60 and 40 mW/cm^2 . The surface morphology of the mesoporous silicon substrates, etched by different illumination steps of 20 mW/cm^2 and 100 mW/cm^2 were characterized by means of SEM top views to evaluate the influence of the illumination steps on porous silicon structures. The multi porous layer is clearly shown in the SEM images, where pores and trenches of different sizes and shapes are formed within the porous matrix. Figure (3), shows the SEM micrograph of (mPsi) sample etched at two etching steps with laser intensities of 40 mW/cm^2 and 20 mW/cm^2 . As shown in the image, a mesoporosity layer has been formed with two different structures: the mud-like structure of connected and non-connected trenches, and the pore-like structure of different pore sizes, formed inside each mud structure. The formation of this complex structure was occurred in the mid-range of porous silicon formation. The increase of illumination intensity leads to a change in the overall structure. The variations in surface morphology of (mPsi) sample etched at four etching steps with laser intensities of 100, 80, 40 and 20 mW/cm^2 are shown in Figures (4 and 5). The top view of the resulting psi layer in Figure (4) presents the formation of two different structures: the first is a mud-like structure of connected and non-connected trenches with the number of trenches and the width of trenches greater than that of the Figure (3). The second structure is a pore-like structure of many small pore sizes. This structure was formed inside each mud-like structure as shown in Figure (5). The formation of this complex structure was occurred in the high-range of porous silicon formation. The distance between the pore-like structure regions for (mPsi) sample etched at two etching steps is in the range $(1-3) \mu\text{m}$ while for (mPsi) sample etched at four etching steps it is about $(3-15) \mu\text{m}$. This increase in the width of the trenches could have been resulted as a result of the illumination intensity increase. This may enhance the silicon dissolution process during the porous formation which leads to the formation of a complex silicon matrix system of different pores and trenches sizes. These pores and trenches are aligned in random directions, with their widths increase with increasing the laser illumination intensity. The explanation of these results is based on the K. Cheah model [11], in which etching process depends on the rate of photo-generation of electron-hole pairs; this rate increase with increasing the illumination intensities.

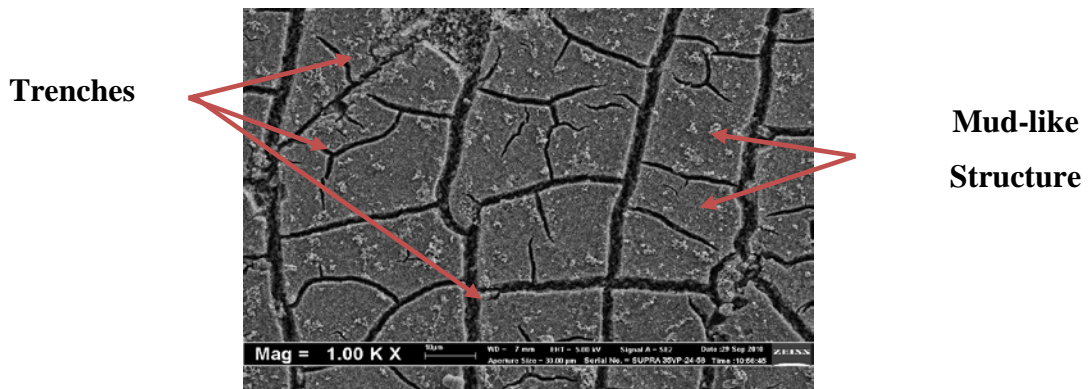


Figure (3), Shows the SEM micrograph of (mPsi) sample etched at two etching steps with laser intensities of 40 mW/cm^2 and 20 mW/cm^2 .

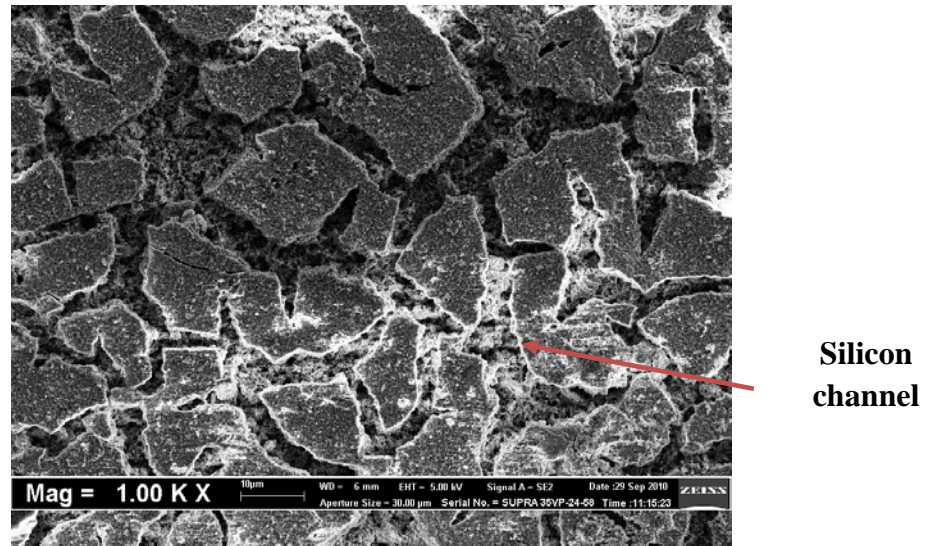


Figure (4) Shows the SEM micrograph of (mPsi) sample etched at four etching steps with laser intensities of $100, 80, 40$ and 20 mW/cm^2 .

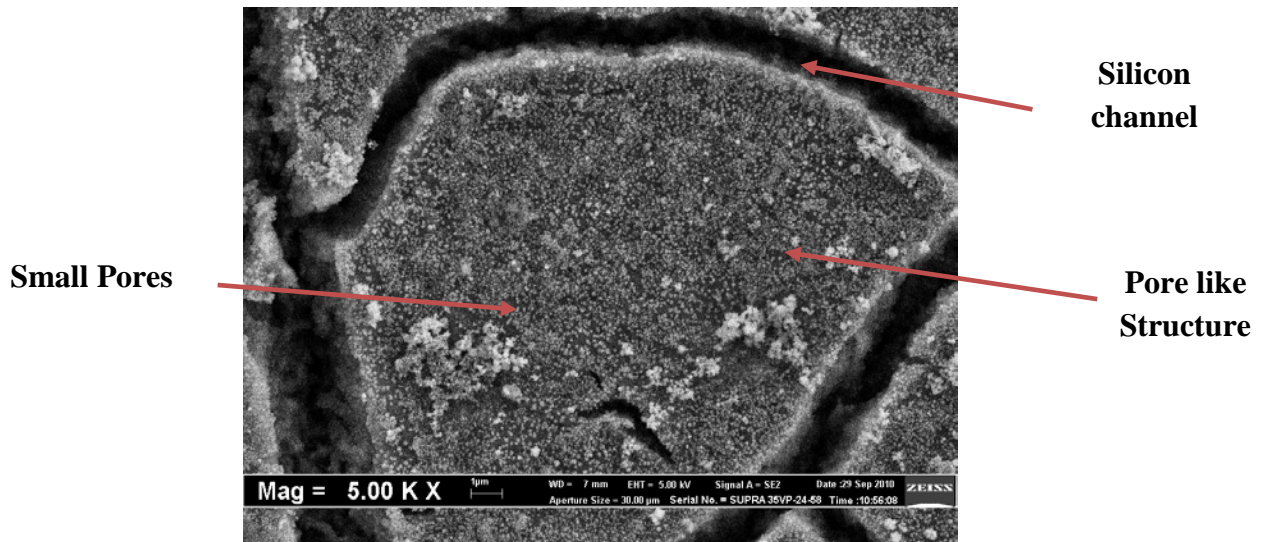


Figure (5) Shows the magnified SEM micrograph of (mPsi) sample etched at four etching steps with laser intensities of $100, 80, 40$ and 20 mW/cm^2 .

The electrical response (I-V characteristics) of the fabricated sensor ambient air and 0.2% ethanol at room temperature is shown in Figure (6). Below 1 Volt forward biasing, the current increased by a factor of 22, while it increased by a factor of 4.5 for the same voltage under reverse biasing. For this reason all measurements were done under forward biasing.

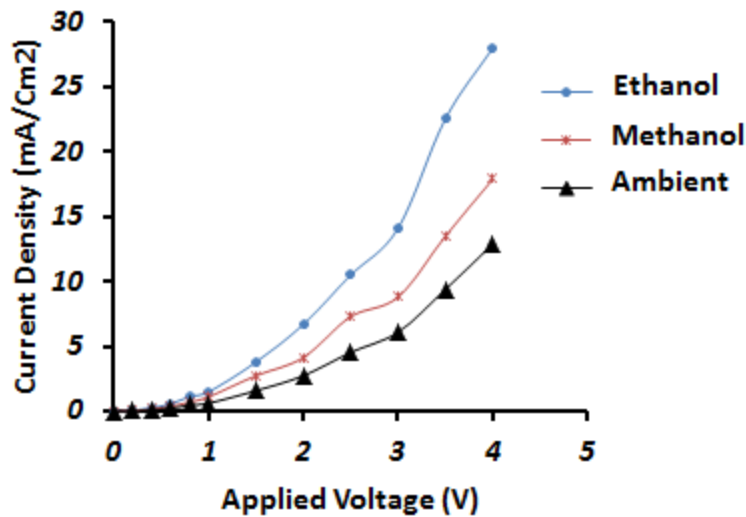


Figure (6), Electrical response (I-V characteristics) of (mPsi) sample etched at two etching steps with laser intensities of 40 mW/cm^2 and 20 mW/cm^2 in the presence ambient air, Ethanol and Methanol.

Figures (6 and 7) illustrate the current response of the fabricated sensor for biasing voltage range of (0-4v) as a function of ethanol and methanol vapors evaporated from 0.2% solution concentration. The Figures show a non-linear response with small slope at 2 volt. When the applied voltage increases above this value, the current increased rapidly to a large value. This rectifying behavior in the current response is due to Schottky junction between the gold thin film and the multi-porous silicon layer. It was found that the electrical response of this sensor for ethanol vapors is higher than that of the methanol. This is probably due to the good absorptivity of the silicon to ethanol than the methanol and this will lead to efficient passivation of the dangling bonds of the porous silicon layer [6]. The (mPsi) sample etched at four etching steps using laser intensities of 100, 80, 40 and 20 mW/cm^2 produced high value of dangling bonds [12]; higher than both of (mPsi) sample etched at two etching steps with laser intensities of 40 mW/cm^2 and 20 mW/cm^2 and the single porosity layer [12]. This increase in dangling bonds may be the reason of high electrical responsively for this vapor sensor compared to other porous silicon vapor sensors [6].

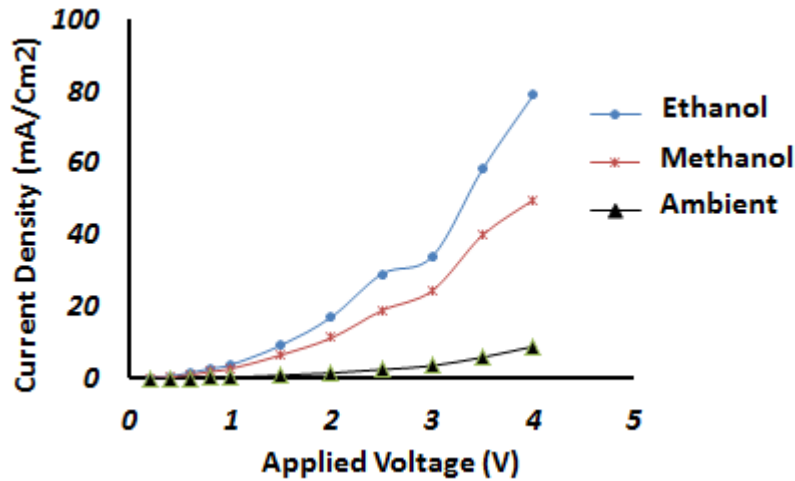


Figure (7), Electrical response (I-V characteristics) of (mPsi) sample etched at four etching steps with laser intensities of 100, 80,40and20 mW/cm²in the presence Ambient air,Ethanol and methanol.

The current flow analysis of the fabricated sensor is based on the morphological nature and the resistivity of the resulting porous silicon with the aid of the model described by M.ben-Chorin et al [13] and the Stievenard and Deremes model [14]. According to M.ben-Chorin et al [13] model, the conductance of the porous silicon layer and hence, the current passing through it is varied with the applied voltage (v), activation energy (Ea) and porous silicon layer parameters like layer thickness (h) and embedding ϵ_r medium in exponential form as shown in equation(3).

$$G(V, T) = G \cdot \exp\left[-\frac{Ea}{KT}\right] \exp\left[\sqrt{\frac{V}{V^*}}\right] \quad \dots (3)$$

Where the value of V^* is given by $\sqrt{V^*} = \frac{KT}{q} \left[\frac{q}{\pi \epsilon \epsilon_r h} \right]^{-\frac{1}{2}}$.

Since the porous silicon is basically a mixture of silicon and embedding medium (air, ethanol, methanol and others) which fills the pores in the porous matrix, therefore, the value of dielectric constant ϵ_r is a function of the porosity of the porous layer (p) according to reference [15].

$$\epsilon_{r_{psi}} = \epsilon_{r_{si}} - p(\epsilon_{r_{si}} - \epsilon_{r_{pore}}) \quad \dots (4)$$

Where $\epsilon_{r_{pore}}$ is the dielectric constant of the embedding medium, the dielectric constant of ethanol and methanol are 24.3 and 33 respectively. For ethanol and methanol vapor, the dielectric constant of porous silicon matrix is higher than that of crystalline silicon and the current passing through the silicon matrix is varying with the concentration of the chemical vapors inside the pores within the matrix structures. The formation of multi porosity psi layer allows forming a pore and trenches of different sizes

and shapes. This will lead to the penetration of chemical vapors inside the matrix better than that the single porosity psi layer. In addition, there will be an increase in the density of the dangling (Si—H) bonds [12] ; these bonds will absorb effectively the organic vapors [6, 16].

CONCLUSIONS

Efficient porous silicon organic vapors sensors have been fabricated by using a multi-porosity porous silicon layer (mPSi) within (Au/mPSi/n-Si/Au) sandwich structures. The multi-porous silicon layer is prepared by laser-assisted etching with step-gradient illumination intensity technique. It was found that the measured I-V characteristics of the sensor have shown rectifying behavior with high sensitivity for the low concentrations of organic vapors. The electrical response of this sensor is attributed to the surface morphology of the (mPSi) and their related parameters.

REFERENCES

- [1]. Canham. L.T, Appl. Phys. Lett. 57, 1046, 1990.
- [2]. Thust M., Schoning M.J, Frohnhoff S, Arens-Fischer R., Kordos P., Luth H., Meas. Sci. Technol. 7, 26, 1996.
- [3]. Schoning M.J, Ronkel F., Crott M, Thust M., Kordos P., Luth H., Electrochim. Acta , 42 , 20, 1997.
- [4]. Kim S.J and Lee S.H., Journal of Korean Physical Society, 44, 1, 167, 2004.
- [5]. Kim S.J., Lee S.H., and Lee C.J., J. Phys. D: Appl. Phys, 34, 3505, 2001.
- [6]. Alwan M Alwan., Eng & Technology Journal 25 , 8 , 2007 .
- [7]. Thonissen M., Berber M.G, Billat S., Arens-Fischer R and ., Luth H., Thin Solid Films 297, 92, 1997.
- [8]. Wang J D., Wang S B., Chou C H ., Thin Solid Films 519, 2313, 2011.
- [9]. Zangoie S., Jansson R. and Arwin H., Mater. Res. Soc. Symp. Proc. 557, 195 (1999).
- [10]. Striemer C.C., Fauchet P.M., Appl. Phys. Lett. 81, 2980 (2002).
- [11]. Cheah K. and C. Choy C., Appl. Phys. 61.45.1995.
- [12]. Alwan M Alwan. and Zahraa S. Ahmed Eng & Technology Journal to (be published)
- [13]. Ben-Chorin M. , Moller F. and Koch F., Phys. Rev. B 49, 2981, 1994.
- [14]. Stievenard D. and Deremes., Appl. Phys. Lett. 67, 11, 1570, 1995.
- [15]. Peng C., Hirschman and K.D and Fauchet P M. J. Appl. Phys, 80 , 295, 1996.
- [16]. M.K. Petra, K. Manzoo, M. Manoth Defence SC. Ence Jonral, 58, 5, 2008